Ups and (Draw)Downs

Tommaso Proietti*

University of Rome "Tor Vergata"

Abstract

The concept of drawdown quantifies the potential loss in the value of a financial asset when it deviates from its historical peak. It plays an important role in evaluating market risk, portfolio construction, assessing risk-adjusted performance and trading strategies. We consider a novel measurement framework that produces, along with the drawdown and its dual (the drawup), two Markov chain processes representing the current lead time with respect to the running maximum and minimum, i.e., the number of time units elapsed from the most recent peak and trough. Together with the distribution of asset returns, they determine the properties of the drawdown and drawup time series, in terms of size, serial correlation, persistence and duration; furthermore, they form the foundation of a new algorithm for dating peaks and troughs of the price process delimiting bear and bull market phases. We then turn our attention to the problem of predicting the drawdown out-of-sample.

Keywords: Financial Time Series; Forecasting Risk Measures; Dating Bear and Bull Markets.

*Address for correspondence: Department of Economics and Finance, University of Rome Tor Vergata, Via Columbia 2, 00133 Rome, Italy. E-mail tommaso.proietti@uniroma2.it.

1 Introduction

In the analysis of financial time series the drawdown measures the potential loss implicit in the current market value of a financial asset with respect to the running maximum value. It provides a path-dependent indicator of downside risk which has become increasingly popular for hedge and mutual funds, commodity trading and insurance; see, among others, ? (?), ? (?, sec. 5), ? (?, p. 78), ? (?), ? (?), and the references therein. ? (?) review the main developments in the literature related to the drawdown. The drawup, the dual process of the drawdown, measures the deviation of the current price from the historical minimum.

The maximum drawdown over a given investment horizon complements classical risk measures; as reported by ? (?), investors assign to it great consideration for evaluting trading strategies and portfolio managers. ? (?, ?) investigated the tail mean of the distribution of maximum drawdowns over finite paths, referred to as Conditional Expected Drawdown; ? (?) studied the Maximum Drawdown at Risk, defined as a quantile of the maximum drawdown distribution. ? (?) introduced a family of risk measures called Conditional Drawdown at Risk (CDaR), representing the tail mean of drawdown distribution, encompassing the average and maximum drawdown, and analyzed its mathematical properties.

In parallel to these developments, the literature has considered replacing the variance in portfolio optimization by risk measures based on the drawdown. Maximization of the expected return of a portfolio under constraints on the drawdown process was pioneered by ? (?) and extended by ? (?). ? (?) consider the problem of minimizing the CDaR of a portfolio subject to a constraint on the expected return. In addition, several drawdown-based performance measures have been developed, the most popular being the Calmar ratio, which is the ratio of excess mean returns to the maximum drawdown of a portfolio. See ? (?, sec. 4.3) for an overview and references. ? (?) discuss the theoretical underpinnings of these measures.

Against this background, the purpose of this paper is to provide a characterization of the drawdown of a discrete time price process, under realistic assumptions concerning the

probabilistic structure of the process. As in ? (?), we adopt the notion of drawdown with a fixed and finite window, depending on a horizon parameter τ, which will be assumed to be fixed and chosen by the investigator, according to the scope of the investment. A key element is the introduction of two adapted processes, measuring respectively the current lead time from the running maximum and minimum. These processes are discrete state first order Markov chains, which, under suitable assumptions on the price process, are homogeneous and ergodic. The time series properties of drawdowns and drawups are dependent upon those of absolute multiperiod returns and the ergodic probabilities of the two Markov chains.

The lead time processes are also at the basis of new dating algorithm for identifying peaks and troughs of the price process delimiting bull and bear market phases. Moreover, their transition probabilities are the essential ingredients for characterizing the duration of drawdown/drawup periods. There is a substantial literature on the problem of dating and characterizing bear and bull markets, see ? (?), ? (?), ? (?), ? (?), ? (?), and on drawdown duration, see ? (?) and the references therein. The paper contributes to this literature by providing a new model-free dating algorithm that is derived in the context of drawdown and drawup measurement.

Subsequently, we address the problem of forecasting the drawdown of a financial asset. Two strategies are considered: one based on direct time series modeling of observed drawdowns, and another that estimates the conditional mean of future drawdowns using simulated future price paths derived from a conditionally heteroscedastic model. Our empirical findings indicate that the latter approach yields a significant improvement in forecast accuracy.

The other original contributions of this paper are the following: (i) we consider the use of daily *high* and *low* prices for determining the upper and lower bound for the drawdown computed on the closing price; (ii) we provide methods for robust estimation of the drawdown, in the presence of microstructure noise.

Our empirical illustrations refer to the S&P500 daily stock market index (closing price) from January 3, 2000, to August 30, 2023, and its components stocks. The time series were downloaded from Yahoo Finance using the `quantmod` R package and the tickers obtained

from Wikipedia's *List of S&P 500 companies*.

The paper has the following structure. The next section defines the drawdown and drawup processes, and related processes, such as the current time distance from the running maximum and minimum. Section 3 illustrates the time series properties of the drawdown. The dating algorithm for bull and bear phases is presented in section 4. Section 5 positions the drawdown as a measure of risk and provides a decomposition of the CDaR that highlights the role of overall risk of an asset and that of the investment horizon. Section 6 looks at the problem of forecasting drawdowns, presenting and comparing direct and indirect approaches. Section 7 works out the lower and upper bound for the drawdown and proposes a denoising estimation strategy based on a parametric lowpass filter. In section 8 we draw our conclusions.

2 Drawdowns and drawups: basic definitions

Let $P_t, t = 0, 1, \ldots, n$, denote the logarithmic price of a financial asset, where t is time in days; we define the log-return at time t as $R_t = P_t - P_{t-1}$, $t = 1, \ldots, n$. The multiperiod (uncompounded) return is defined as $R_t(i) = P_t - P_{t-i} \equiv \sum_{k=0}^{i-1} R_{t-k}$. Obviously, $R_t(1) = R_t$ and for convention we extend the definition to $i \in 0, 1, \ldots, \tau, \tau \in \mathbb{Z}^+$, by setting $R_t(0) = 0$.

Definition 1. *The τ-maximum process, M_t^+, and the associated τ-drawdown process, D_t, are defined respectively as*

$$M_t^+ = max\{P_t, P_{t-1}, \ldots, P_{t-\tau}\}, \quad D_t = M_t^+ - P_t, \quad t = \tau, \tau+1, \ldots, n. \tag{1}$$

The lead time with respect to the running maximum defines the discrete random process S_t^+, with $\tau + 1$ states $S_t^+ = i$, if $M_t^+ = P_{t-i}$, $i = 0, \ldots, \tau$.

Definition 2. *The τ-minimum process, M_t^-, and the associated τ-drawup process, U_t, are defined respectively as*

$$M_t^- = \min\{P_t, P_{t-1}, \ldots, P_{t-\tau}\}, \quad U_t = P_t - M_t^-, \quad t = \tau, \tau+1, \ldots, n. \tag{2}$$

The lead time with respect to the running minimum defines the discrete random process S_t^-, with $\tau + 1$ states $S_t^- = i$, if $M_t^- = P_{t-i}$, $i = 0, \ldots, \tau$.

M_t^+ defines a random lagged value of P_t, while S_t^+ counts the time units separating the current value from the τ-maximum; M_t^-, and the related processes, are obtained by applying the max-filter to the sign reversed price series, after a sign change, e.g., $M_t^- = -\max\{-P_{t-i}, i = 0, 1, \ldots, \tau\}$.

Definitions 1 and 2 depend on the horizon τ, which determines the size and the dynamics of the drawdown: if $D_t(\tau)$ denotes the drawdown as a function of τ, $D_t(\tau^*) \geq D_t(\tau)$, for $\tau^* > \tau$. This follows immediately from $\max\{P_t, P_{t-1}, \ldots, P_{t-\tau}\} \leq \max\{P_t, P_{t-1}, \ldots, P_{t-\tau^*}\}$. Similar properties hold for U_t. We assume that τ is selected a priori by the analyst, according to a desired or typical duration of a position or investment. Interesting horizons are $\tau = 5, 10, 15, 22, 65$, corresponding to weekly, bi-weekly, tri-weekly, monthly and quarterly horizons.

Figure 1 shows realizations of the aforementioned processes. The observed logarithmic price, denoted as p_t, represents the natural logarithm of the daily S&P 500 stock market index, available from January 3, 2000, to August 31, 2023. Its time series is graphed in the top panel, covering the sub-period from January 3, 2023, to August 30, 2023, for visibility, along with the realization of the maximum and minimum process, $m_t^+ = \max\{p_{t-j}, j = 0 \ldots, \tau\}$, and $m_t^- = \min\{p_{t-j}, j = 0 \ldots, \tau\}$, for $\tau = 22$. The interval (m_t^-, m_t^+), often referred to as the *price channel* in the financial practice, is a measure of local range and volatiliy. The central panel shows the drawdown $d_t = m_t^+ - p_t$ and the drawup $u_t = p_t - m_t^-$, while the bottom panel displays the realized values of the current lead time with respect to the running maximum (s_t^+) and the running minimum (s_t^-).

Table 1 provides some descriptive statistics concerning the drawdown and drawup, and the lead time with respect to the τ maxima and minima, for the S&P500 series starting from January 2000; the values of τ considered are 22 and 65. The distribution of drawdowns is characterized by larger dispersion (in terms of range, interquartile range and standard deviation), skewness and kurtosis, than that of drawups. The mean and median drawup values are larger, instead. On average, drawups are higher and less influenced by extreme values compared to drawdowns. As for the lead time processes, they reveal that the drawdowns of the SP500 index have shorter duration: the median lead time with respect to the 22 days running minimum is 16, as opposed to 6 time units, which is the

Figure 1: Logarithm of S&P500 closing price (January 3, 2023 - August 30, 2023). Top panel: Series (p_t), τ-maxima (m_t^+) and minima (m_t^-) for $\tau = 22$. Central panel: drawdown (d_t) and drawup (u_t). Bottom panel: current lead time from maximum (s_t^+) and minimum (s_t^-).

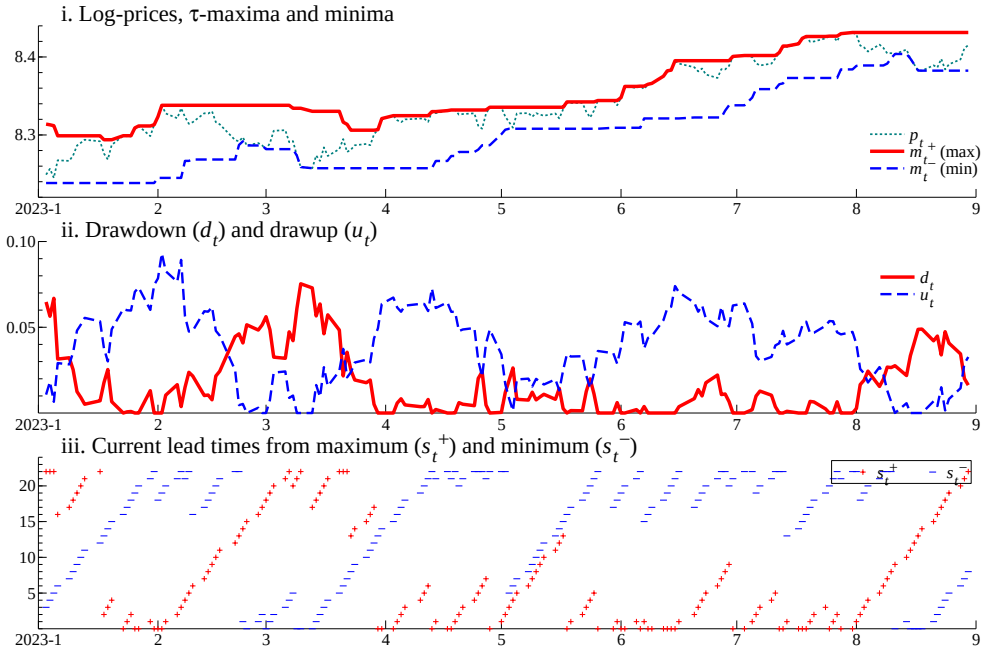

Table 1: S&P500 closing price (January 3, 2000 to August 30, 2023). Descriptive statistics for the drawdown (d_t) the drawup (u_t), the lead time with respect to the running maxima (s_t^+) and minima (s_t^-).

	$\tau = 22$				$\tau = 65$			
	d_t	u_t	s_t^+	s_t^-	d_t	u_t	s_t^+	s_t^-
min	0.000	0.000	0.000	0.000	0.000	0.000	0.000	0.000
$q_{0.25}$	0.002	0.015	1.000	5.000	0.004	0.041	3.000	20.000
median	0.012	0.032	6.000	14.000	0.021	0.068	16.000	45.000
$q_{0.75}$	0.036	0.051	16.000	20.000	0.060	0.098	45.000	60.000
max	0.411	0.251	22.000	22.000	0.547	0.368	65.000	65.000
mean	0.026	0.037	8.563	12.653	0.044	0.074	23.854	39.280
stand. dev.	0.038	0.031	7.813	7.811	0.061	0.051	22.659	21.985
skewness	3.238	1.713	0.463	-0.314	2.648	1.442	0.552	-0.441
kurtosis	19.553	8.267	1.711	1.614	12.737	7.145	1.803	1.782

value recorded for s_t^+. Increasing the horizon to $\tau = 65$ leads to an increase in the size of both d_t and u_t and a reduction of the skewness and kurtosis; the median lead times are also subject to a proportionate increase.

3 Time series properties of the drawdown

Suppose that the τ-maximum (τ-minimum) occurs at time $t - i$. This corresponds to the event $S_t^+ = i$ ($S_t^- = i$), $i \leq \tau$, for which $P_t < P_{t-i}$ ($P_t > P_{t-i}$), so that the drawdown (drawup) equals $|R_t(i)| = P_{t-i} - P_t$. Therefore, the drawdown and drawup are the following measurable transformations of the sequence $\{P_{t-j}, j = 0, 1, \ldots, \tau\}$:

$$D_t = \sum_{i=0}^{\tau} I(S_t^+ = i)|R_t(i)|, \quad U_t = \sum_{i=0}^{\tau} I(S_t^- = i)|R_t(i)|, \tag{3}$$

where $I(\cdot)$ is the indicator function, taking value one if the argument is true and zero otherwise, and we recall having posited $R_t(0) = 0$. The event $S_t^+ = i$ occurs when $P_{t-i} > P_{t-j}$, for $j \neq i, j = 0, \ldots, \tau$, equivalently,

$$\{R_t(i) < 0, R_{t-1}(i-1) < 0, \ldots, R_{t-i+1}(1) < 0, R_{t-i} > 0, R_{t-i}(2) > 0 \ldots, R_{t-i}(\tau - i) > 0\}.$$

On the contrary, $S_t^- = i$ occurs when $P_{t-i} < P_{t-j}, j = 0, \ldots, \tau, j \neq i$, or equivalently when

$$\{R_t(i) > 0, R_{t-1}(i-1) > 0, \ldots, R_{t-i+1}(1) > 0, R_{t-i} < 0, R_{t-i}(2) < 0 \ldots, R_{t-i}(\tau - i) < 0\}.$$

Therefore, D_t and U_t result from applying non-linear filters to the past and current logarithmic returns. Consequently, their characteristics are contingent upon the joint distribution of past and current returns. We will confine our focus to processes satisfying the following assumption.

Assumption 1. *$\{R_t, t = 1, \ldots, n\}$ is strictly stationary with absolutely continuous marginal distribution function $F(x)$, with continuous density $f(x)$, satisfying $E(|R_t|^r) < \infty$ for some $r > 2$. Moreover, it is strongly mixing of size $-r/(r-2)$, i.e., $\alpha_m = O(m^{-s})$, $s > r/(r-2)$.*

Recall that $\{R_t, t \in \mathbb{Z}\}$ is α-mixing (?, ?, Ch. 14) if $\lim_{m\to\infty} \alpha_m = 0$, where α_m is the mixing coefficient, defined as

$$\alpha_m = \sup_{B\in\mathscr{F}_{-\infty}^{t}, C\in\mathscr{F}_{t+m}^{\infty}} |P(B \cap C) - P(B)P(C)|,$$

and $\mathscr{F}_t^s, t < s$ is the σ-field generated by $\{R_t, R_{t+1}, \ldots, R_s\}$. We also say that $\{R_t, t \in \mathbb{Z}\}$ is α-mixing of size $-g_0$, $g_0 > 0$, if $\alpha_m = O(m^{-g}), g > g_0$.

Assumption 2. *$\tau \geq 1$ is a fixed positive integer.*

Under Assumptions 1-2 the processes S_t^+ and S_t^- are first order homogeneous Markov chains with ergodic probabilities $\pi_i^+ = P(S_t^+ = i)$ and $\pi_i^- = P(S_t^- = i)$, respectively, for $i = 1, \ldots, \tau$. Homogeneity is implied by the assumption of strict stationarity, by which the joint distribution of $\{R_{t-j}, 0 \geq j \geq \tau\}$ does not depend on t. The continuity condition prevents the occurrence of ties ($R_t(i) = 0$ has zero probability).

The transition probabilities, $p_{ij}^+ = P(S_{t+1}^+ = j | S_t^+ = i), p_{ij}^- = P(S_{t+1}^- = j | S_t^+ = i), i, j = 0, 1, \ldots, \tau$, are obtained uniquely from the joint distribution of the $\tau+1$ consecutive returns $\{R_{t+1-k}, k = 0, \ldots, \tau\}$, see ? (?, sec. 3) for details. The transition matrix of S_t^+ takes the form:

$$T^+ = \begin{pmatrix} p_{00}^+ & p_{01}^+ & 0 & \ldots & 0 & 0 \\ p_{10}^+ & 0 & p_{12}^+ & \ldots & 0 & 0 \\ p_{20}^+ & 0 & 0 & \ddots & 0 & 0 \\ \vdots & \vdots & \ldots & \ddots & \ddots & \vdots \\ p_{\tau-1,0}^+ & 0 & 0 & \cdots & 0 & p_{\tau-1,\tau}^+ \\ p_{\tau 0}^+ & p_{\tau 1}^+ & p_{\tau 2}^+ & \cdots & p_{\tau,\tau-1}^+ & p_{\tau\tau}^+ \end{pmatrix}. \tag{4}$$

From state i, $i = 0, \ldots, \tau - 1$, the only admissible transitions are to 0 or $i+1$: for instance, in the drawdown case, either $P_{t+1} > P_{t-i}$, and thus a transition is made to state 0, or $P_{t+1} < P_{t-i}$. Therefore, the first $\tau - 1$ rows of the transition matrix have only two nonzero entries: p_{i0}^{+} and $p_{i,i+1}^{+} = 1 - p_{i0}^{+}$. On the contrary, from state τ a transition can be made to any other state. The transition matrix of the Markov chain S_t^{-} is derived similarly, and has the same lower Hessenberg structure as (4), with the 0's located in the same position.

Given the representation (3), it has been proven in ? (?) that under Assumptions 1-2 the drawdown process D_t is weakly stationary with mean $\mu_D = \sum_{i=0}^{\tau} \pi_i^{+} \mathrm{E}(|R_t(i)|)$, variance $\mathrm{Var}(D_t) = \sum_{i=0}^{\tau} \left[\mathrm{Var}(|R_t(i)|) + \mathrm{E}(|R_t(i)|)^2\right] \pi_i^{+} - \mu_D^2$, and autocovariance function

$$\mathrm{Cov}(D_t, D_{t+k}) = \sum_{i=0}^{\tau} \sum_{j=0}^{\tau} \left[\mathrm{Cov}(|R_t(i)|, |R_{t+k}(j)|) + \mathrm{E}(|R_t(i)|)\mathrm{E}(|R_t(j)|)\right] p_{ij}^{+(k)} \pi_i^{+} - \mu_D^2, \quad (5)$$

where $p_{ij}^{+(k)} = P(S_t^{+} = j | S_{t-k}^{+} = i)$, $i, j = 0, \ldots, \tau$, are the elements of the k-period transition matrix $[T^{+}]^k$. Moreover, the strong-mixing regularity condition of Assumption 1 implies that the autocovariance sequence is absolutely summable, since $|\mathrm{Cov}(D_t, D_{t+k})| = O\left(|k|^{-(1+\epsilon)}\right), \epsilon > 0$.

Similar properties hold for the drawup process U_t, which has mean $\mu_U = \sum_{i=0}^{\tau} \mathrm{E}(|R_t(i)|)\pi_i^{-}$ and $\mathrm{Cov}(U_t, U_{t+k})$ taking the same expression as (5) with $p_{ij}^{+(k)}$ replaced by the elements of the k-period transition matrix of the chain S_t^{-}, and π_i^{+} replaced by π_i^{-}.

As it is clear from (3), D_t and U_t are characterized by strong serial dependence and are cross-correlated, being a mixture of absolute multiperiod returns for all horizons from 1 to τ. As such, they are a manifestation of the volatility of asset returns.

3.1 Example: Gaussian random walk

As mentioned in the introduction, several contributions have characterized aspects of the probability distribution of a drawdown in a continuous time setting, when the data generating process is a Wiener or a Levy process. We complement those results by illustrating, in discrete time, the properties of the drawdown (mean, variance and temporal persistence), and the associated Markov Chain S_t^{+} (ergodic and transition probabilities), when logarithmic prices are generated as a Gaussian random walk with drift. The main

driver of those features is the drift of one-period returns relative to their standard deviation, also known as the Sharpe ratio.

Let $P_t = P_{t-1} + \mu + \epsilon_t$, $\epsilon_t \sim$ i.i.d. $\mathrm{N}(0, \sigma^2)$. Suppose $\tau = 1$. Then D_t can take only two values, 0 and $|R_t|$, with probabilities $\pi_0^+ = \Phi(\mu/\sigma)$ and $\pi_1^+ = 1 - \pi_0$, respectively, where $\Phi(z)$ is the cumulative distribution function of a standard normal random variate. Using the properties of the folded normal distribution,

$$\mu_D = \Phi\left(-\frac{\mu}{\sigma}\right)\left[\sigma\sqrt{\frac{2}{\pi}}e^{-0.5\mu^2/\sigma^2} + \mu\left\{1 - 2\Phi\left(-\frac{\mu}{\sigma}\right)\right\}\right].$$

Moreover, D_t is serially uncorrelated, and $\mathrm{Var}(D_t) = (\sigma^2 + \mu^2)\Phi\left(-\frac{\mu}{\sigma}\right) - \mu_D^2$. Finally, the transition probabilities are equal to the unconditional ones, e.g., $p_{00}^+ = p_{10}^+ = \Phi\left(\frac{\mu}{\sigma}\right)$.

For $\tau > 1$, D_t is a moving average process of order $\tau - 1$, and $p_{00}^+ = \Phi(\mu/\sigma)$; if $\mu = 0$, this is also equal to $p_{\tau\tau}^+$, i.e., the first and last same state probabilities are both equal to 0.5. The remaining marginal and transition probabilities of S_t^+ are evaluated analytically with the support of the algorithms provided by ? (?) for the multivariate folded normal distribution.

Table 2 presents the ergodic probabilities π_i^+, the same-state transition probabilities p_{00}^+ and $p_{\tau\tau}^+$, the unconditional mean and variance of D_t, the values of its autocorrelation function at lags 1, 5, and 10, as the Sharpe ratio, μ/σ, varies from -2.5 to 2.5; the horizon parameter is set equal to $\tau = 22$. In the zero drift case the chain has a symmetric probability distribution, $\pi_i^+ = \pi_{\tau-i}^+$, and the only admissible same state transition probabilities (p_{00}^+ and $p_{\tau\tau}^+$) are both equal to 1/2. The expected drawdown is obviously larger when the drift is negative and decreases monotonically as the Sharpe ratio increases.

As μ/σ increases, π_0^+ tends to 1, the expected gap decreases towards zero and its variance decreases: when the drift is positive and high, relative to σ, S_t^+ tends to be in state 0 (π_0^+ is close to 1). Also, the persistence of D_t varies inversely with the Sharpe ratio.

3.2 Estimation of marginal and transition probabilities

Given a time series of logarithmic prices, the estimation of the marginal and transition probabilities of the Markov chains S_t^+ and S_t^- takes place as follows. Let us define the indicator function $I_{it}^+ = I(S_t^+ = i)$, taking value 1 if $S_t^+ = i$ and zero otherwise. Denoting

Table 2: Characteristics of the Markov chain S_t^+ and of drawdown process D_t, when $\tau = 22$ and prices are generated by the Gaussian random walk process $P_t = P_{t-1} + \mu + \sigma\epsilon_t, \epsilon_t \sim$ i.i.d. $\mathrm{N}(0, \sigma^2)$, as a function of the Sharpe ratio μ/σ.

	Values of μ/σ										
	-2.5	-2.0	-1.5	-1.0	-0.5	0.0	0.5	1.0	1.5	2.0	2.5
μ_D	54.98	43.95	32.86	21.67	10.18	2.34	1.02	0.36	0.14	0.05	0.02
$\mathrm{Var}(D_t)$	22.04	22.09	22.19	22.39	21.86	5.54	3.88	1.03	0.37	0.14	0.05
ACF(1)	0.95	0.95	0.95	0.94	0.94	0.86	0.78	0.49	0.26	0.10	0.02
ACF(5)	0.77	0.77	0.76	0.75	0.71	0.49	0.34	0.05	0.03	-0.02	0.00
ACF(10)	0.54	0.54	0.54	0.52	0.47	0.22	0.12	0.00	0.01	-0.03	0.00
π_0^+	0.00	0.00	0.00	0.00	0.00	0.12	0.53	0.80	0.93	0.98	0.99
π_1^+	0.00	0.00	0.00	0.00	0.00	0.06	0.16	0.13	0.06	0.02	0.01
π_2^+	0.00	0.00	0.00	0.00	0.00	0.05	0.09	0.04	0.01	0.00	0.00
π_3^+	0.00	0.00	0.00	0.00	0.00	0.04	0.06	0.02	0.00	0.00	0.00
π_4^+	0.00	0.00	0.00	0.00	0.00	0.04	0.04	0.01	0.00	0.00	0.00
π_5^+	0.00	0.00	0.00	0.00	0.00	0.03	0.03	0.00	0.00	0.00	0.00
$\vdots$	$\vdots$	$\vdots$	$\vdots$	$\vdots$	$\vdots$	$\vdots$	$\vdots$	$\vdots$	$\vdots$	$\vdots$	$\vdots$
π_{17}^+	0.00	0.00	0.00	0.00	0.03	0.03	0.00	0.00	0.00	0.00	0.00
π_{18}^+	0.00	0.00	0.00	0.01	0.04	0.04	0.00	0.00	0.00	0.00	0.00
π_{19}^+	0.00	0.00	0.00	0.02	0.06	0.04	0.00	0.00	0.00	0.00	0.00
π_{20}^+	0.00	0.00	0.01	0.04	0.09	0.05	0.00	0.00	0.00	0.00	0.00
π_{21}^+	0.01	0.02	0.06	0.13	0.16	0.06	0.00	0.00	0.00	0.00	0.00
π_{22}^+	0.99	0.98	0.93	0.80	0.53	0.12	0.00	0.00	0.00	0.00	0.00
p_{00}^+	0.00	0.01	0.08	0.19	0.31	0.50	0.69	0.84	0.93	0.98	0.99
$p_{22,22}^+$	0.99	0.98	0.93	0.84	0.69	0.50	0.31	0.19	0.08	0.01	0.00

the number of joint occurrences of $S_t^+ = i$ and $S_{t+1}^+ = j$ as

$$n_{ij}^+ = \sum_{t=\tau+1}^{n} I_{i,t-1}^+ I_{jt}^+,$$

the transition probabilities of the Markov chain S_t^+ are estimated by

$$\hat{p}_{ij}^+ = \frac{n_{ij}^+}{n_{i.}^+},$$

where $n_{i.}^+ = \sum_{j=0}^{q} n_{ij}^+$. The estimator of the marginal probabilities is

$$\hat{\pi}_i^+ = \frac{n_{i.}^+}{\sum_{j=0}^{\tau} n_{j.}^+}, \quad i = 0, 1, \ldots, \tau.$$

The large sample properties of these estimators have been derived in ? (?). Analogous estimators are adopted for the marginal and transition probabilities of S_t^-.

For the S&P500 time series, for $\tau = 22$, $\hat{\pi}_0^+ = 0.1839$ and $\hat{\pi}_0^- = 0.0826$, meaning that the proportion of time units for spent at the maximum (minimum) of the last 22 observations is 18.4% (8.3%). The probability of a continuation of the maximum is $\hat{p}_{00}^+ = 0.5005$, while that of a minimum is smaller ($\hat{p}_{00}^- = 0.4265$).

4 A dating algorithm for turning points, bear and bull phases

Dating business and financial cycles has a long-standing tradition in economics, tracing back to the early work of Burns and Mitchell at the National Bureau of Economic Research (NBER), see ? (?). The NBER maintains an authoritative chronology of the US business cycle, based on the consensus of a committee of expert economists, which identifies peak and trough dates that delineate alternating periods of expansion and recession. This chronology is qualitative, relying on expert judgment informed by a number of macroeconomic indicators.

Dating algorithms are instead data-driven methods that identify turning points according to deterministic or probabilistic rules. An early instance is ? (?). The algorithm introduced in this Section aims at classifying bull and bear phases of the financial cycle within this tradition.

Dating algorithms are intrinsically non-parametric. An alternative model-based approach to identify the phases of the business cycle is provided by the class of Markov switching (MS) models, according to which the mean of a representative indicator of aggregate economic activity, such as gross domestic product real growth, takes different values in expansion and recession. See ? (?) and ? (?). Financial applications are mostly related to the identification of periods of low and high volatility.

The Markov chains S_t^+ and S_t^- can be used to date peaks and troughs of a stock index, delimiting bear and bull phases of the market. A peak marks the inception of a bear market phase, which is terminated by a trough. A bull phase is entered after a trough and is terminated by a peak.

The dating algorithm has two steps that are hereby described.

1. Identification of candidate turning points. Let $k \leq \tau$ denote a positive integer determining the "isolation" of peaks and troughs.

   - A candidate peak at time t is identified by the event

   $$\{S_{t-j}^{-} > 0\} \cap \{S_t^{+} = 0\} \cap \{S_{t+j}^{+} = j\}, \;\; j = 1, 2, \ldots, k.$$

   In words, a necessary condition for the occurrence of a peak is that a local maximum is found at time t ($S_t^{+} = 0$), and the current price is above the next k prices ($P_t > P_{t+j}, j = 1, \ldots, k$), while prices have been moving upwards from their historical minimum for the previous k periods, $(S_{t-j}^{-} > 0), j = 1, 2, \ldots, k$.

   - A candidate trough at time t is identified by the event

   $$\{S_{t-j}^{+} > 0\} \cap \{S_t^{-} = 0\} \cap \{S_{t+j}^{-} = j\}, \;\; j = 1, 2, \ldots, k.$$

   In words, at time t a local minimum occurs ($S_t^{-} = 0$), and the current price lies below the next k prices ($P_t < P_{t+j}, j = 1, \ldots, k$), while prices are moving downwards from their τ-maximum $(S_{t-j}^{+} > 0), j = 1, 2, \ldots, k$.

2. Enforce the alternation of turning points. The candidate turning points do no necessarily alternate, i.e., nothing prevent that two or more consecutive peaks are identified after a trough, and viceversa. Consecutive candidate peaks (troughs) are eliminated in a sequential manner, by selecting the one for which the logarithmic price is larger (smaller).

The dating algorithm depends crucially on the horizon τ and considers in the first step $2k + 1$ consecutive values of (S_t^{+}, S_t^{-}), centred at t. The choice of the isolation parameter k affects predominantly the number of preliminary turning points that are identified: too large a k would lead to discard candidate turning points that do not comply with the isolation property required of a peak or a trough. Having a smaller k leads to a greater number of candidates and is potentially less dangerous, as irrelevant turning points would be eliminated in the second step. However, k enforces a minimum duration constraint on the subsequent bear and bull phase. In general, the dating algorithm is relatively

insensitive to the choice of k, which induces minor difference only during very prolonged bear and bull phases; we found that choosing $k \approx \tau/3$ provides a reasonable solution.

The dating algorithm has been applied to the S&P500 index and to 484 series with complete observations starting not later than January 2016. The horizon that was used is $\tau = 65$ (a quarter of a year of daily observations) and k was set equal to 22. Figure 2 plots, along with the series, the turning points (vertical lines) and the bear phases identified for the index (shaded areas). The series in blue is the diffusion index of a bear phase, i.e., the proportion of individual stock series that are in a bear phase at a particular time. This is tipically larger than 1/2 during episodes like the great financial crisis, the Covid-19 crisis, and the energy crisis triggered by the Ukraine war.

The duration of the phases depends on the drift and the variability of the market: during the first years of the 2000's prolonged bear phases prevailed, in association with a downturn of the market.

Obviously, the characterization of bear and bull phases is bound up with the definition of the horizon τ. This is an essential ingredient. An investor rebalancing the portfolio every quarter would look at the phases identified for $\tau = 65$; one rebalancing every month would consider $\tau = 22$.

For the S&P500 index the probability of being in a bear (bull) state is estimated to be equal to 31.66% (68.34%). A bear (bull) phase is typically associated with $D_t > 0$ ($U_t > 0$), although there are instances in which a minor trough (peak), occurring before a major one, could be eliminated by the above procedure. This occurs rarely: while U_t is found to be always positive during a bull phase, $D_t = 0$ during a bear phase was found in 4 cases out of 1864. Moreover, it does not hold that D_t (U_t) is identically equal to zero during a bull (bear) phase. A positive drawdown can be found after a trough, i.e. during a bull phase, if the trough occurs after $r < \tau$ time units after a previous peak (a peak is sometimes evocatively described as a *high water mark*). Actually, $P(U_t > 0|\text{Bear})$ and $P(D_t > 0|\text{Bull})$ are estimated equal to 90.34% and 80.91%, respectively.

In other words, the emerging and the persistence of positive drawdowns (drawups) serve to identify a candidate peak (trough), but the indicator of a positive drawdown (drawup) does not depend perfectly on the bear and bull phase.

Figure 2: S&P500 logarithmic prices (red), bull (white) and bear (grey) phases and bear diffusion index (blue), based on 484 component series.

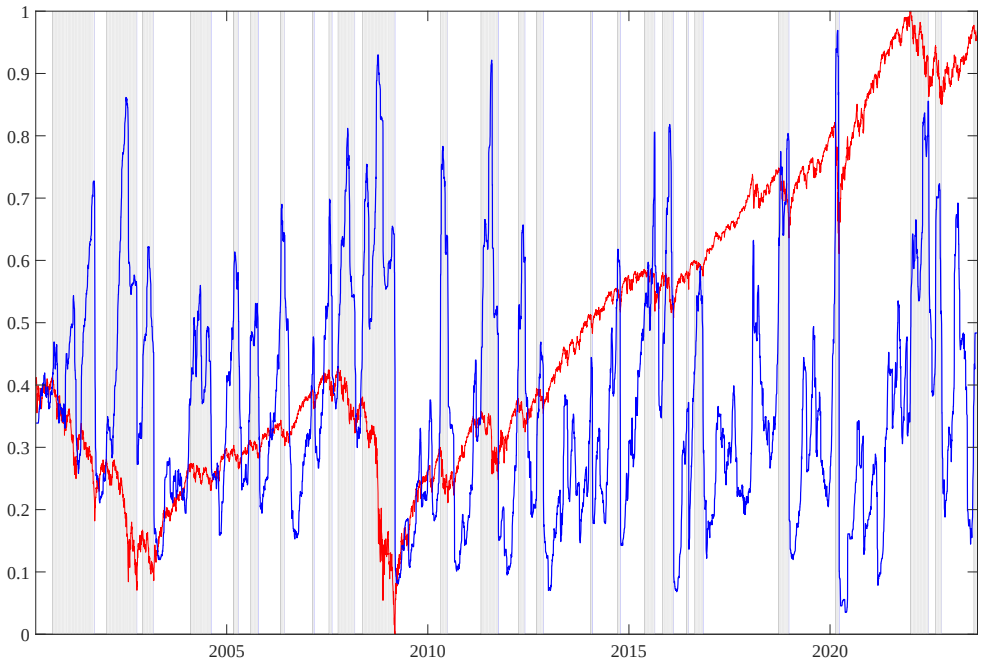

4.1 Drawdown and drawup duration

The processes S_t^+ and S_t^- are at the basis of two constructed random variables measuring the duration of a rally of positive drawdowns and drawups.

Let us define the random variable $\mathscr{D}_d$ taking values $\mathscr{D}_d = k$, $k = 0, 1, \ldots, \tau$, if, after being in a peak at time t, the price process lies below P_t in the subsequent k times and peaks again at time $t+k+1$; under such circumstances, positive drawdowns have persisted for k periods. We posit, for $k \leq \tau$,

$$\begin{aligned} P(\mathscr{D}_d = k) &= P(S^+_{t+k+1} = 0, S^+_{t+k} = k, \ldots, S^+_{t+1} = 1 | S^+_t = 0) \\ &= \begin{cases} p^+_{00}, & k = 0, \\ p^+_{01} p^+_{12} \cdots p^+_{k-1,k} p^+_{k0}, & 1 \leq k \leq \tau. \end{cases} \end{aligned} \tag{6}$$

For $k > \tau$, we can only provide the survival probability $P(\mathscr{D}_d > \tau) = 1 - \sum_{k=0}^{\tau} P(\mathscr{D}_d = k)$. If the chain has transition probabilities satisfying $p^+_{i,i+1} = 1 - p^+_{00}$, for positive integer i and $\tau \to \infty$, $\mathscr{D}_d$ is a geometric random variable, i.e., $P(\mathscr{D}_d = k) = p^+_{00}(1 - p^+_{00})^k$, $k \geq 0$. The probability distribution of $\mathscr{D}_d$ can be estimated once the transition probabilities of

the chain S_t^+ are estimated according to section 3.2.

In a similar way, we can construct a variable for the duration of drawups, $\mathscr{D}_u$, taking the value k if, after the occurrence of a trough at time t (i.e., $S_t^- = 0$), P_{t+j} lies above P_t for all $1 \leq j \leq k$, and a new local minimum is reached at time $t + k + 1$.

Table 3 reports the drawdown and drawup duration probabilities $P(\mathscr{D}_d = k)$ and $P(\mathscr{D}_u = k)$ for selected values of k, along with the corresponding survival probabilities, estimated from the Markov chains s_t^+ and s_t^- with $\tau = 22$ adapted to the S&P500 time series. Interestingly, the comparison of the survival functions $P(\mathscr{D}_d > k)$ and $P(\mathscr{D}_u > k)$ shows that the distribution of the duration of drawups ($\mathscr{D}_u$) dominates stochastically that of drawdowns, i.e., once a positive drawups phase is entered, there is a higher probability of remaining in the same phase, with respect to a positive drawdowns phase. The survival

Table 3: SP500 index 2000-01-03 to 2023-08-30 ($n = 4026$). Probability distribution of the duration of a drawdown ($\mathscr{D}_d$) and a drawup ($\mathscr{D}_u$).

k	$P(\mathscr{D}_d = k)$	$P(\mathscr{D}_d > k)$	$P(\mathscr{D}_u = k)$	$P(\mathscr{D}_u > k)$
0	0.5005	0.4995	0.4265	0.5735
1	0.1568	0.3427	0.1605	0.4130
2	0.0830	0.2597	0.0533	0.3597
3	0.0347	0.2249	0.0450	0.3147
4	0.0289	0.1961	0.0358	0.2790
5	0.0252	0.1708	0.0182	0.2608
6	0.0242	0.1467	0.0095	0.2513
7	0.0186	0.1280	0.0125	0.2388
8	0.0103	0.1177	0.0122	0.2266
9	0.0071	0.1106	0.0100	0.2166
10	0.0075	0.1032	0.0055	0.2111
11	0.0044	0.0988	0.0040	0.2071
12	0.0056	0.0932	0.0062	0.2009
13	0.0033	0.0899	0.0023	0.1986
14	0.0037	0.0863	0.0032	0.1954
15	0.0046	0.0816	0.0041	0.1913
16	0.0022	0.0794	0.0019	0.1894
17	0.0020	0.0774	0.0049	0.1845
18	0.0029	0.0745	0.0043	0.1802
19	0.0025	0.0720	0.0030	0.1772
20	0.0014	0.0706	0.0040	0.1731
21	0.0017	0.0689	0.0026	0.1706
22	0.0042	0.0647	0.0060	0.1646

probability after 22 days is less than 7% in the case of a drawdown, whereas it is about

17% for a drawup.

5 Some stylized facts

The time series of drawdowns, d_t, and drawup, u_t, with $\tau = 22$ have been computed for the $N = 501$ constituent stocks of S&P500, along with the states s_t^+ and s_t^-, which measure the distance in time units from the running maximum and the running minumum price, respectively.

To analyze risk diversification and investigate the influence of systemic factors on risk, or for pairs trading, it is essential to assess the association among individual stocks. This raises the question concerning which drawdown correlation measure should be considered, in the light of the constraints on the values of both d_t and u_t - limited to nonnegative real values - and the presence of a non-negligible proportion of zero observations, quantified by $\hat{\pi}_0^+$ and $\hat{\pi}_0^-$. Moreover, the serial correlation in d_t and u_t may lead to an overassessment of the stocks' comovements.

Focusing exclusively on the time period from January 3, 2000, to August 30, 2023, and narrowing our analysis to the subset of 381 data series with complete observations, in Figure 3 we present a comparison of five pairwise association measures. These measures are computed for two generic stocks, labeled as r and s, and encompass the following: (i) Pearson's correlation between the time series d_{rt} and d_{st}. (ii) Spearman's rank correlation coefficients between the time series d_{rt} and d_{st}, which is the correlation of the probability integral transform of the drawdown series. (iii) Pearson's correlation coefficient between the values of s_{rt}^+ and s_{st}^+, treating the variables as quantitative. (iv) Cramér's V,

$$V_{rs} = \sqrt{\frac{\chi^2_{rs}}{\tau(n-\tau)}}, \chi^2_{rs} = \sum_{i=0}^{\tau}\sum_{j=0}^{\tau} \frac{\left(n^+_{ij,rs} - n^+_{i.,rs}n^+_{.j,rs}/(n-\tau)\right)^2}{n^+_{i.,rs}n^+_{.j,rs}/(n-\tau)},$$

where $n^+_{ij,rs}$ is the number of times $s_t^+ = i$ for stock r and $s_t^+ = j$ for stock s. This amounts to treating the current lead time from the maximum as a nominal variable. (v) Goodman-Kruskal *gamma* index (?, ?, sec. 2.4.4),

$$\gamma_{rs} = \frac{C_{rs} - D_{rs}}{C_{rs} + D_{rs}}, \quad C_{rs} = \sum_{i=0}^{\tau}\sum_{j=0}^{\tau} n^+_{ij,rs}\left(\sum_{h>i}\sum_{k>j} n^+_{hk,rs}\right), D_{rs} = \sum_{i=0}^{\tau}\sum_{j=0}^{\tau} n^+_{ij,rs}\left(\sum_{h>i}\sum_{k<j} n^+_{hk,rs}\right).$$

Figure 3: Cross-sectional distribution and relation between measures of pairwise association between 381 stocks making up the S&P500 index (January 3, 2020 - August 30, 2023).

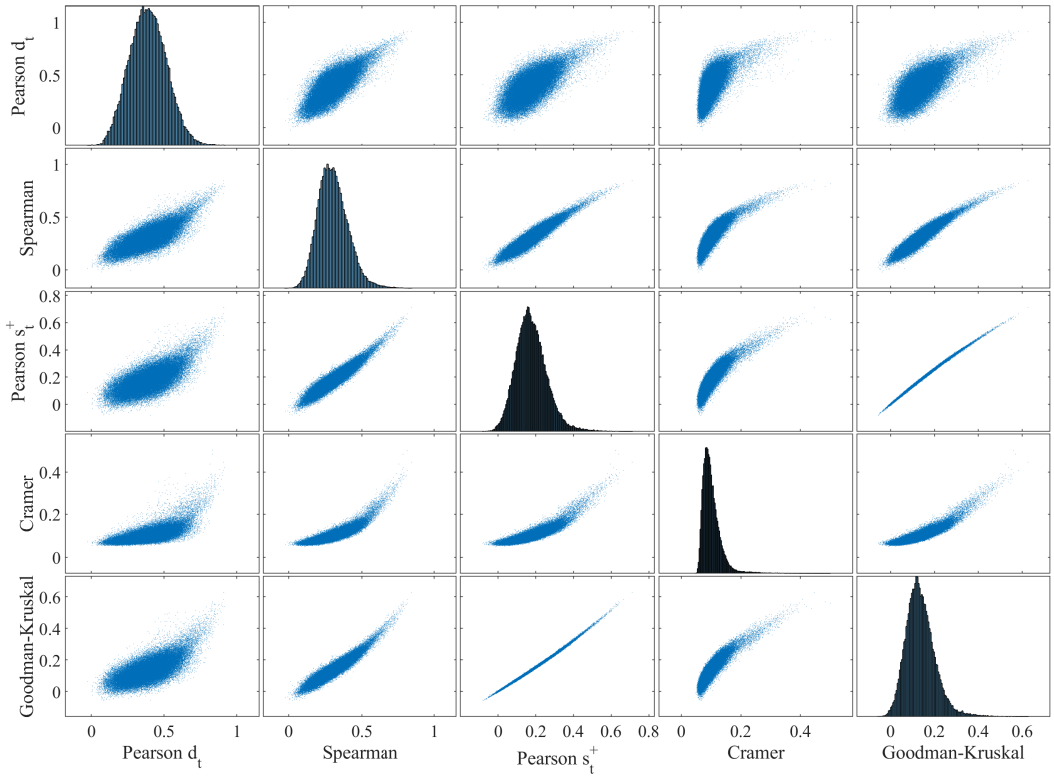

In this context, C_{rs} represents the number of concordances, and D_{rs} represents the number of discordances; this amounts to treating the current lead time from the maximum as an ordinal variable. All of these measures yield values within the range of -1 to 1, with the exception of Cramér's V, which falls within the 0 to 1 range.

Figure 3 illustrates the marginal cross-sectional distribution of the 72,390 pairwise coefficients, and their bivariate scatterplots. Pearson's drawdown correlation has the largest variability and least concordance with the other measures; on the contrary, Spearman's rank correlation shows high coherence with the association measures based on s_t^+. Concerning the latter, there is an almost perfect one-to-one correspondence between γ_{rs} and Pearson's correlation based on s_t^+; finally, we would probably dismiss Cramér's V on the grounds that it is not a signed measure.

? (?), see also ? (?), define the conditional drawdown at risk (CDaR) at the level α as

the average of the $(1-\alpha)$ largest drawdowns:

$$\text{CDaR}(\tau,\alpha) = \frac{1}{(1-\alpha)n}\sum_{t=1}^{n} d_t I(d_t \geq q_\alpha),$$

where q_α denotes the α-quantile of the τ-drawdown distribution. The CDaR encompasses the mean drawdown, which arises for $\alpha = 0$, the median drawdown ($\alpha = 0.5$), and the maximum drawdown ($\alpha = 1$). The conditional drawup at risk (CUaR) is defined similarly, $\text{CUaR}(\tau,\alpha) = \frac{1}{(1-\alpha)n}\sum_{t=1}^{n} u_t I(u_t \geq q_\alpha)$. Both $\text{CDaR}(\tau,\alpha)$ and $\text{CUaR}(\tau,\alpha)$ are increasing in both arguments. We shall return to this issue later.

The correlation heatmap in figure 4 presents the cross-sectional association, across $N = 381$ constituent stocks of S&P500, of a number of risk measures, $\text{CDaR}(22,0)$, $\text{CDaR}(22,0.5)$, $\text{CDaR}(22,1)$, $\text{CUaR}(22,0)$, $\text{CUaR}(22,0.5)$, $\text{CUaR}(22,1)$, characteristics of asset returns, namely average returns $\hat{\mu} = \frac{1}{n}\sum_{t=1}^{n} r_t$ and their standard deviation, $\hat{\sigma} = \sqrt{\frac{1}{n}\sum_{t=1}^{n}(r_t - \hat{\mu})^2}$, two performance measures, namely the Sharpe ratio, $\hat{\mu}/\hat{\sigma}$, and the Calmar ratio, $\hat{\mu}/\text{CUaR}(22,1)$, and a set of characteristics of the observed Markov chains s_t^+ and s_t^-: the estimated probability of being in state zero (the current value coincides with the historical maximum/minimum), $\hat{\pi}_0^+$ and $\hat{\pi}_0^-$, respectively, the same state transition probabilities $\hat{p}_{00}^+$ and $\hat{p}_{00}^-$, and the bull and bear survival probabilities at $\tau = 22$ days. The measure of association adopted is Spearman's rank correlation, which is invariant to monotonic transformations of the variables.

Strong associations exist among the risk measures (CDaR and CUaR), which are also strongly and positively correlated with the standard deviation. Similarly, the performance measures (Sharpe and Calmar) exhibit a significant positive correlation, with coefficient 0.96. These metrics show positive relationships with $\hat{\mu}$ but negative associations with the risk measures. The persistence of a bear state, as measured by $\hat{\pi}_0^-$, $\hat{p}_{00}^-$, and $P(\mathscr{D}_d > 22)$, demonstrates a positive correlation with the risk metrics and a negative one with the performance metrics. Conversely, when examining variables that express the persistence of a drawup state, such as $\hat{\pi}_0^+$, $\hat{p}_{00}^+$, and $P(\mathscr{D}_u > 22)$, the direction of the association is reversed.

We conclude this section with an analysis of the dependence of the CDaR for the i-th asset, denoted $\text{CDaR}_i(\tau,\alpha)$, $i = 1, 2, \ldots, N$, on the horizon τ and the level α. While α

Figure 4: Heatmap of the pairwise Spearman's rank correlation coefficients of selected features of τ-drawdown and τ-drawup time series, based on $N = 361$ stocks with complete observations for the period Jan. 2000-Aug. 2023, and $\tau = 22$.

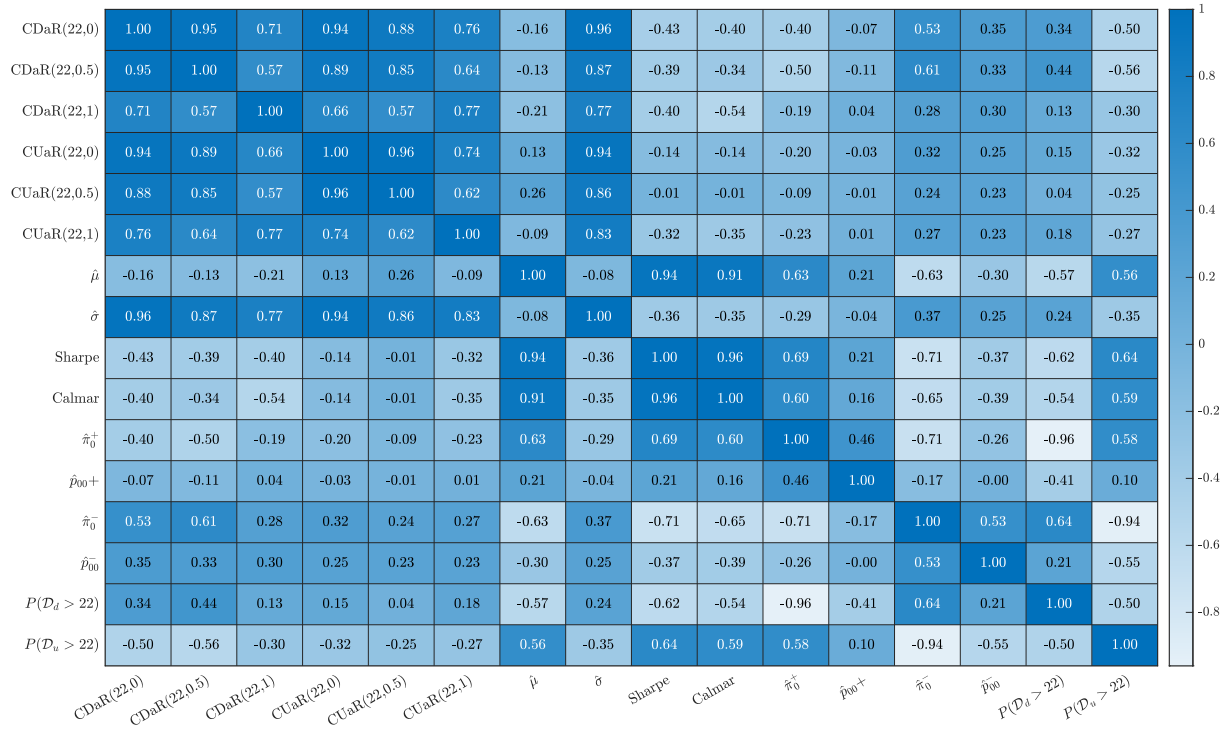

varies within the range of [0,1], the Conditional Drawdown at Risk (CDaR) assesses the tail mean of the distribution of drawdowns. Also, when τ is increased for a specific α, the tail mean increases, as drawdown is a strictly increasing function of τ.

In Figure 5, you can observe the contour plots of $\mathrm{CDaR}(\tau, \alpha)$ for the stocks of two competing firms belonging to the Consumer Staples sector, labelled A and B. The left panel displays the logarithmic price of these stocks. It is evident that stock A experiences larger drawdowns, especially in the initial decade of the sample period and at the outset of the Covid-19 pandemic crisis. During the global financial crisis, the drawdowns are of a comparable magnitude. As a result, the drawdown of firm A dominates stochastically that of firm B for all choices of τ and α.

By performing the rank 1 singular value decomposition of the matrix whose (k, l) element is $\mathrm{CDaR}_i(\tau_k, \alpha_l)$, with $\tau_k = k$, $k = 1, \ldots, 65$, and $\alpha_l = l/41, l = 0, 2, \ldots, 40$, we obtain the following factorization:

$$\mathrm{CDaR}_i(\tau_k, \alpha_l) = \lambda_i \theta_i(\tau_k) \nu_i(\alpha_l) + \epsilon_i, i = 1, \ldots, N,$$

where λ_i is the first singular value of the CDaR matrix, $\theta_i(\tau_k)$ is the k-th element of the first left singular vector, and $\nu_i(\alpha_l)$ is the l-th element of the first right singular vector. The above factorization captures the bulk of the variability of $\mathrm{CDaR}_i(\tau_k, \alpha_l)$: the customary goodness of fit statistic for the rank 1 least squares approximation of the matrix of CDaR values, given by the ratio λ_i^2 to sum of the squares of all the singular values, is never below 0.99 for all stocks.

The scalar λ_i can be interpreted as the overall risk factor for the i-th asset. Its cross-sectional distribution across the 381 individual stocks is estimated by the histogram and the kernel density shown in the left panel of figure 6; the values range from a minimum of 3.65 to a maximum of 18.48; the median and the mean are respectively 7.71 and 8.25, with a standard deviation equal to 2.85.

The loadings $\theta_i(\tau_k), \tau_k = 1, \ldots, 65$, provide the τ-profile of risk, expressing the increase of risk with the length of the time horizon of the investment. They are displayed in the central panel of figure 6, each curve referring to a different stock. The τ-profile is increasing in τ according to the power law $\theta_i(\tau_k) = a_i \tau_k^{\beta_i}$; when the coefficients β_i are estimated by regressing $\log(\theta_i(\tau_k))$ on $\log(\tau_k)$, the estimates average out to 0.52 with a standard

Figure 5: Daily price series of stocks A and B (logarithms, Jan. 3, 2000 - Aug. 30, 2023, left panel). Contour plots of $\mathrm{CDaR}_i(\tau, \alpha)$, $i = \{A, B\}$, for $1 \leq \tau \leq 65$ and $0 \leq \alpha \leq 1$ (right panel).

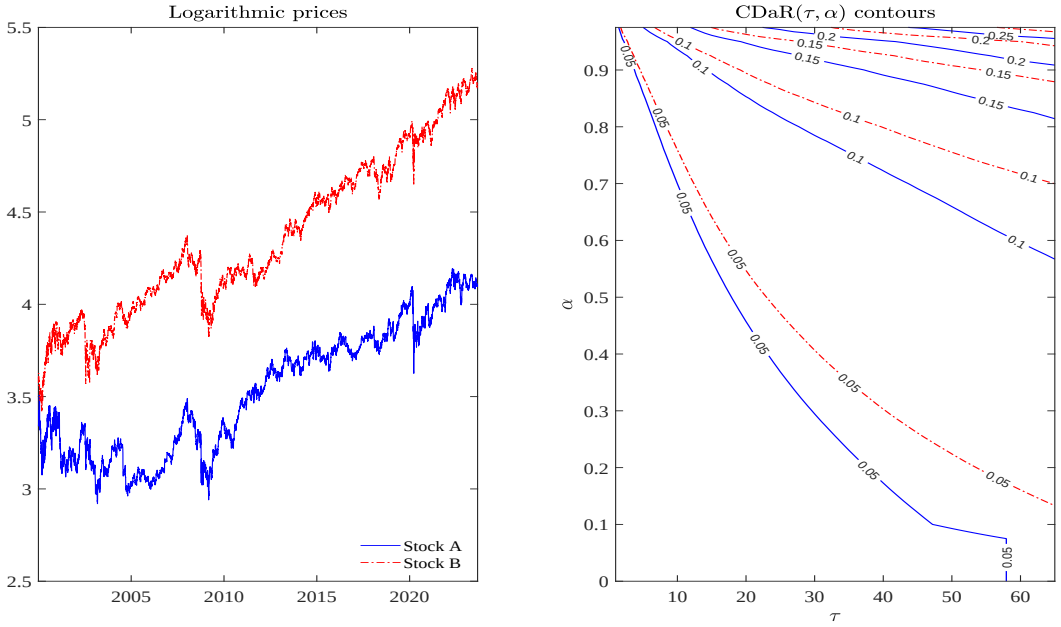

deviation equal to 0.04, which shows that the profile displays some heterogeneity across the stocks. As a result the square-root-of-τ rule for characterizing how risk increases with the investment horizon can be used only as a first approximation. It should be noticed that the τ-profiles cross, meaning that some stocks can be relatively more risky at longer horizons than they are at shorter ones. Most curves cross around the horizon corresponding to 41 days.

The α-profile of risk is informative on the tail behaviour of the distribution of drawdown. It increases with α at a faster rate and it is constant for low values of α depending on the frequency of observed zero drawdowns, which varies from stock to stock. Most individual curves cross at $\alpha = 0.87$. More risky stocks (characterized by larger λ_i values, coloured in red) tend to have lower (higher) profile curves for α smaller (larger) than this threshold.

Figure 6: CDaR factorization. Distribution of the risk factors λ_i for 381 stocks (left panel). τ-profile of risk (central panel). The colour of the individual curves ranges from dark green to red according to the increasing values of λ_i. α-profile of risk (right panel).

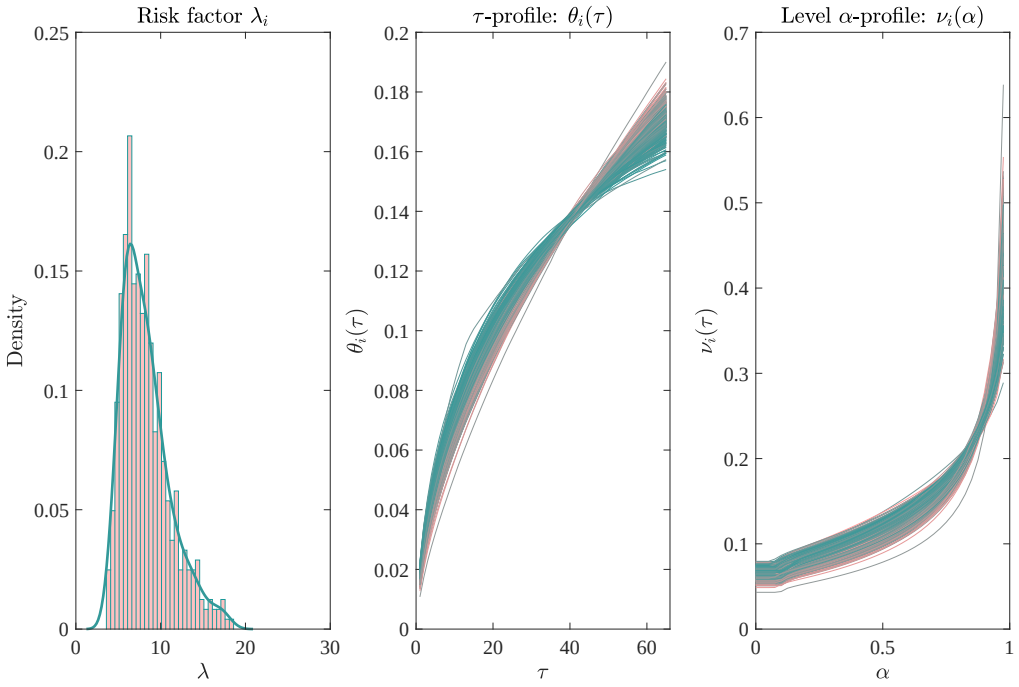

6 Forecasting Drawdowns

We address the issue of forecasting D_{t+h} at time t using the information available at that time. Given that the drawdown is a measurable transformation of current and past prices, the question arises as to whether it is it more efficient predicting directly the drawdown from a time series of past drawdowns, or indirectly from the price forecasts, by comparing the predicted price to the running τ-maximum of the price series augmented by its forecasts.

In the latter case, assuming a quadratic loss function, the optimal h-step-ahead predictor of prices is the conditional expectation of P_{t+h}, given the information available at time t, denoted $\mathrm{E}_t(P_{t+h})$, which is obtained by cumulating all forecastable returns,

$$\mathrm{E}_t(P_{t+h}) = p_t + \sum_{j=1}^{h} \mathrm{E}_t(R_{t+j}).$$

Suppose that asset returns are generated by a generalized autoregressive conditionally heteroscedastic (?, ?, GARCH) process: $R_t = \mu + \sigma_t \varepsilon_t$, where, if $\mathscr{L}(0,1)$ denotes the distribution of a continuous random variable with mean 0 and unit variance, $\varepsilon_t \sim$ i.i.d. $\mathscr{L}(0,1)$, and

$$\sigma_t^2 = \omega + \alpha(R_{t-1} - \mu)^2 + \beta\sigma_{t-1}^2,$$

where that $\omega, \alpha > 0$, $\beta \geq 0$ and $\mathrm{E}\{\log(\alpha\varepsilon_t^2 + \beta)\} < 0$, under which assumptions R_t is strictly stationary (?, ?).

Drawdown forecasting can be made by sequential Monte Carlo, drawing samples from the predictive distribution of prices, and thus of the drawdown, and finally taking the average of the predicted particles. If we let $p_{t+j}^{(i)}, j = 1, 2, \ldots h$, denote the i-th sample path of future prices at time t, a draw from the predictive distribution of drawdowns is

$$d_{t+h}^{(i)} = \max\{p_{t+h-j}^{(i)}, j = 0, 1, \ldots, \tau\} - p_{t+h}^{(i)}$$

where, if $h < \tau$, $p_{t+h-j}^{(i)} = p_{t+h-j}$.

If M denote the number of independent paths, $i = 1, \ldots, I$, the final h-step-ahead forecast of the drawdown is obtained by averaging the I draws:

$$\hat{d}_{t+h|t} = \frac{1}{I} \sum_{i=1}^{I} d_{t+h}^{(i)}. \tag{7}$$

Assuming that the parameters of the GARCH model and μ are known at time t, the draws $d_{t+h}^{(i)}$ are obtained by the following simulation scheme:

- For $i = 1, 2, \ldots, I$,
  - Set $r_{t|t}^{(i)} = r_t$, $\sigma_{t|t}^{2(i)} = \sigma_t^2$.
  - For $j = 1, 2, \ldots, h$, draw $r_{t+j|t}^{(i)} \sim \mathscr{L}(\mu, \sigma_{t+j|t}^{2(i)})$, where

$$\sigma_{t+j|t}^{2(i)} = \omega + \alpha(r_{t+j-1|t}^{(i)} - \mu)^2 + \beta\sigma_{t+j-1|t}^{2(i)}.$$

- Evaluate $p_{t+h|t}^{(i)} = p_t + \sum_{k=1}^{h} r_{t+k|t}^{(i)}$.
- Set $d_{t+h|t}^{(i)} = \max\{p_{t+h-j|t}^{(i)}, j = 0, 1, \ldots, \tau\} - p_{t+h|t}^{(i)}$.

The direct approach is based on a forecasting model for the d_t time series. We consider five different predictors.

- The direct predictor of D_{t+h} based on fitting an ARMA model, selected according an information criterion such as Akaike's, to the series d_t (D-ARMA).
- The direct exponential smoothing predictor of D_{t+h}, based on fitting an ARIMA(0,1,1) model by maximum likelihood (D-ARIMA(0,1,1)).
- The direct predictor of D_{t+h} based on fitting the Heterogeneous Autoregressive (HAR) model proposed by ? (?), such that

$$D_t = m + \beta_1 D_{t-1} + \beta_2 \bar{D}_{5,t-1} + \beta_3 \bar{D}_{22,t-1} + e_t,$$

  where e_t is assumed to be white noise and $\bar{D}_{rt} = \sum_{j=0}^{r-1} D_{t-j}$ (D-HAR).
- Recalling (3), the conditional predictor

$$\mathrm{E}(D_{t+h}|S_t^+ = i, \mathscr{F}_t) = \sum_{j=0}^{\tau} p_{ij}^{+(h)} \tilde{\mu}_{t+h|t}(j),$$

  is based on the forecast of the state indicators $I(S_{t+h}^+ = j|S_t^+ = i)$ through the h-step transition probabilities $p_{ij}^{+(h)}$ and those of the j-step-ahead returns $\tilde{\mu}_{t+h|t}(j) = \mathrm{E}_t|R_{t+h}(j)|$. The latter will be obtained fitting HAR models to the $|R_t(j)|$ series, $j = 1, \ldots, \tau$ (C-HAR).

- The conditional factor predictor is based on the same logic, but obtains the multistep forecasts $\tilde{\mu}_{t+h|t}(j) = \mathrm{E}_t|R_{t+h}(j)|$ by a factor model, as

$$\tilde{\mu}_{t+h|t}(j) = a_1\hat{f}_{1,t+h} + a_2\hat{f}_{2,t+h} + a_3\hat{f}_{3,t+h},$$

  where the factors and their loadings are estimated by performing a principal component analysis of the absolute multistep returns series, $|r_t(j)|$, and predicted by fitting independent HAR models to the first three principal factors, which are sufficient to represent most of the variation of $|r_t(j)|$ (C-Factor HAR).

Table 4 presents the outcomes of a rolling forecasting experiment designed to forecast the S&P500 drawdown with horizon $\tau = 22$. This experiment involved employing rolling window of $T = 4,000$ observations as a training sample for estimating the forecasting models. Drawdown forecasts were made for up to 22 days in advance, and were compared to the actual values. Subsequently, the earliest observation was removed from the training set, a new observation was added at the end, and the out-of-sample forecasting exercise was repeated. This process was reiterated until the end of the sample period was reached. In total, the experiment generated 1,824 forecast errors for each forecast horizon, ranging from 1 to 22 days, over the test period spanning from November 25, 2015, to July 31, 2023. The indirect predictor (7) is based on $I = 1,000$ particles.

The second column of Table 4 reports the root mean square error (RMSE) of the particle Monte Carlo (MC) predictor (7), which serves as a reference:

$$\mathrm{RMSE}(h) = \sqrt{\sum_{t=n-T}^{n-22}(\hat{d}_{t+h|t} - d_{t+h})^2}, h = 1, \ldots, 22.$$

The remaining columns display the ratio of the RMSE of the five direct predictors to that of the particle MC predictor. Values greater (smaller) than one indicate a worse (better) predictive performance. Notably, among the direct predictors, Direct-HAR (D-HAR) is characterized by the best forecasting performance, yielding the smallest RMSE for forecast horizons from $h = 17$ to $h = 22$. However, for shorter horizons, the particle MC predictor stands out prominently as the most accurate option.

The question of whether the particle MC forecasting method yields a significant improvement in predictive accuracy is examined using the ? (?) test for equal predictive

accuracy, applied against each of the direct forecasting methods. Table 5 reports the values of the test statistic under a quadratic loss function. Under the null hypothesis, the test statistic follows a standard normal distribution, and positive values indicate that the direct predictor listed in the column has a higher average loss than the particle MC predictor.

To estimate the long-run variance of the loss differential, $h+1$ autocovariances were employed. The results support and complement the preceding discussion, providing evidence in favor of the particle MC method: the Diebold-Mariano test rejects the null hypothesis of equal predictive accuracy in favor of the particle MC method at horizons up to at least 10 (one-sided test, critical value 1.64). At longer horizons, the null of equal accuracy is generally not rejected. An exception occurs at horizon 22, where the null is rejected in favor of the alternative that the D-HAR method is more accurate.

A major advantage of the particle MC method is the availability of interval and density estimates of the drawdown resulting from the sequential simulation experiment. Figure 7 shows one instance of the rolling forecasting experiment, specifically related to predicting the drawdown for the 22 days spanning from February 28, 2023, to March 29, 2023, based on the 4,000 observations available on February 27. The figure displays the forecasts (7), along with the first and third quartiles of the predictive distribution and the 95% predictive interval, showing that the observed drawdowns fell within it.

7 Robustness and Microstructure noise

7.1 Upper and lower bounds for the drawdown

So far we have been considering the drawdown that an investor faces at the closing of the market. This is an understatement of the drawdown that is faced in real life, as it does not take into account the intradaily variability of prices. The availability of the time series of daily maximum (*high*) and minimum (*low*) prices recorded in day t, denoted P_t^+ and P_t^-, respectively, enables the computation of lower and upper bounds for the drawdown.

The upper bound, D_t^+, is obtained from the time series of daily *high* by applying the maximum filter in Definition 1 to the series P_t^+ of price *high*, and comparing the daily *low*

Table 4: Root mean square error (RMSE) of the particle Monte Carlo predictor $\hat{d}_{t+h|t} = \frac{1}{I}\sum_{i=1}^{I} d_{t+h}^{(i)}$ and relative RMSE of five alternative direct predictors of the S&P500 drawdown.

	RMSE	Relative Root Mean Square Error				
Horizon	Particle MC	D-ARMA	D-ARIMA(0,1,1)	D-HAR	C-HAR	C-Factor HAR
1	0.0115	1.3850	1.4056	1.3766	1.9117	1.9117
2	0.0148	1.3380	1.3740	1.3293	2.0792	2.0792
3	0.0181	1.2443	1.2952	1.2375	2.0911	2.0911
4	0.0208	1.1831	1.2500	1.1788	2.0821	2.0821
5	0.0228	1.1643	1.2460	1.1616	2.0403	2.0403
6	0.0248	1.1178	1.2133	1.1171	1.9280	1.9280
7	0.0260	1.1365	1.2496	1.1365	1.8541	1.8541
8	0.0279	1.0984	1.2237	1.0988	1.6993	1.6993
9	0.0289	1.1112	1.2537	1.1108	1.5970	1.5970
10	0.0306	1.0878	1.2429	1.0864	1.4687	1.4687
11	0.0320	1.0776	1.2474	1.0759	1.3724	1.3724
12	0.0333	1.0679	1.2518	1.0655	1.2985	1.2985
13	0.0346	1.0483	1.2434	1.0454	1.2361	1.2361
14	0.0356	1.0432	1.2516	1.0396	1.2004	1.2004
15	0.0366	1.0270	1.2448	1.0222	1.1680	1.1680
16	0.0373	1.0237	1.2550	1.0184	1.1510	1.1510
17	0.0382	1.0117	1.2546	1.0060	1.1335	1.1335
18	0.0389	1.0023	1.2569	0.9960	1.1189	1.1189
19	0.0397	0.9908	1.2559	0.9841	1.1036	1.1036
20	0.0403	0.9812	1.2560	0.9742	1.0909	1.0909
21	0.0408	0.9745	1.2591	0.9671	1.0784	1.0784
22	0.0410	0.9682	1.2586	0.9604	1.0719	1.0719

price, denoted P_t^-, to the running τ-maximum of P_t^+:

$$D_t^+ = \max\{P_{t-i}^+, i = 0, 1, \ldots, \tau\} - P_t^-.$$

The lower bound, D_t^-, is the drawdown faced by the investor who sells at the current *high*, P_t^+, a stock bought at the historical maximum *low* (this can be negative, hence we take the largest between this drawdown and zero):

$$D_t^- = \max\left\{\max\{P_{t-i}^-, i = 0, 1, \ldots, \tau\} - P_t^+, 0\right\}.$$

It follows directly from $P_t^- \leq P_t \leq P_t^+$ that $D_t^- \leq D_t \leq D_t^+$.

Figure 8 displays the upper (solid blue line) and lower (solid green line) bounds for the drawdown d_t (dotted red line) evaluated for the closing price in the period Jan. 3, 2023 - Aug. 30, 2023. The range of values around d_t depends not only on the

Table 5: Diebold-Mariano test statistics for the null of equal forecast accuracy under quadratic loss. The distribution of the test statistic is standard normal.

Horizon	D-ARMA	D-ARIMA(0,1,1)	D-HAR	C-HAR	C-Factor HAR
1	5.93	5.28	5.85	8.12	8.12
2	4.75	4.17	4.64	5.79	5.79
3	3.95	3.66	3.88	4.91	4.91
4	3.25	3.24	3.27	4.34	4.34
5	2.54	3.03	2.59	3.95	3.95
6	2.16	2.82	2.21	3.65	3.65
7	2.08	2.81	2.12	3.30	3.30
8	1.91	2.49	1.97	3.12	3.12
9	1.93	2.44	1.97	2.88	2.88
10	1.72	2.23	1.76	2.72	2.72
11	1.61	2.12	1.64	2.53	2.53
12	1.45	2.02	1.46	2.34	2.34
13	1.18	1.91	1.17	2.18	2.18
14	1.01	1.85	0.99	2.00	2.00
15	0.71	1.78	0.63	1.91	1.91
16	0.59	1.77	0.50	1.82	1.82
17	0.32	1.74	0.18	1.78	1.78
18	0.07	1.74	-0.13	1.76	1.76
19	-0.29	1.72	-0.58	1.69	1.69
20	-0.64	1.72	-1.05	1.64	1.64
21	-0.89	1.72	-1.38	1.50	1.50
22	-1.12	1.69	-1.69	1.40	1.40

daily price range, $P_t^+ - P_t-$, but also on the maximum historical range, $\max\{P_{t-i}^+, i = 0, 1, \ldots, \tau\} - \max\{P_{t-i}^-, i = 0, 1, \ldots, \tau\}$.

7.2 Price discreteness

Observed high, low, and closing prices are multiple of a tick size, say one cent, so that their values are rounded. As a result, (multi-)period returns can be zero, whenever they fall below half a cent, with the consequence that more than one local maxima or minima can be present. We break the ties at random by running the maximum and minimum filters on the series p_t contaminated by a tiny error, drawn at random from a Gaussian distribution with mean zero and standard deviation 10^{-15}. This noise contamination is purely instrumental to tie breaking and neither affects the reliability of the methods nor contradicts the robust estimation approach of the next section.

Figure 7: S&P500 drawdown series ($\tau = 22$, dotted red line), January 3 - March 29, 2023, and out-of-sample forecasts.

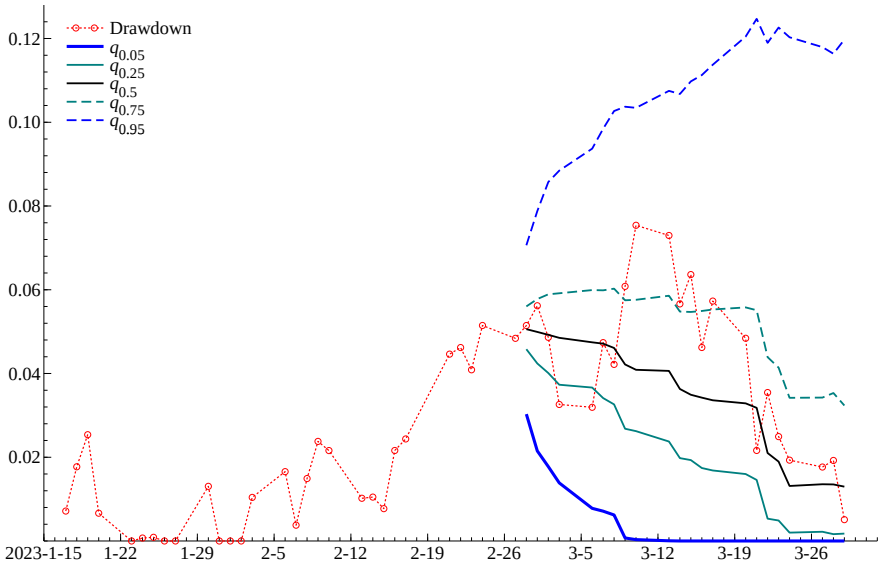

Figure 8: Upper and lower bounds for the drawdown of S&P500 closing logarithmic price (January 3, 2023 - August 30, 2023).

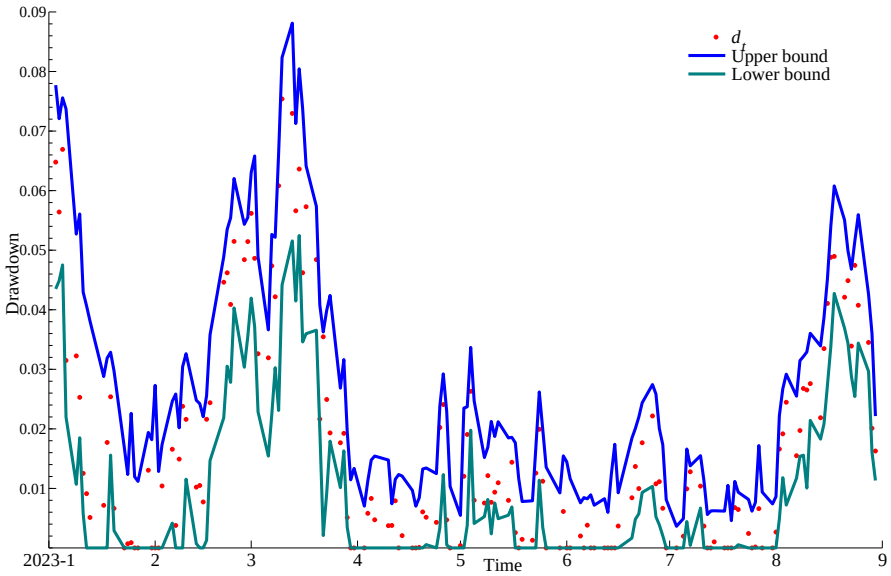

7.3 Robust estimation

Robust drawdown estimation deals with abstracting from irrelevant price variability, e.g., induced by microstructure noise, in the assessment of risk. This notion is inherently different from statistical robustness, which deals with reducing the influence of large values on the inferences. In our framework large drawdowns should not be discounted, actually representing a manifestation of risk.

? (?) introduced the notion of ϵ-drawdown, a measure ignoring variation below a certain magnitude. Hereby we consider a different approach which aims at measuring the drawdown abstracting from high-frequency noise in price movements, which is responsible for the identification of minor peaks and troughs. This is achieved by a parametric low-pass filter applied to P_t, filtering out high-frequency components.

Suppose that prices can be modelled by the ARIMA process

$$P_t = P_{t-1} + \mu + \frac{\theta(L)}{\phi(L)}\xi_t, \quad \xi_t \sim \mathrm{WN}(0, \sigma^2),$$

where $\phi(L) = 1 - \sum_{j=1}^{p} \phi_j L^j$ is a p-th order autoregressive polynomial in the lag operator L, such that $L^k y_t = y_{t-k}$, $\phi(L) \neq 0 \iff |L| \leq 1$ and $\theta(L) = 1 + \sum_j \theta_j L^j$, $\theta(L) \neq 0 \iff |L| \leq 1$ (the latter two conditions ensure stationarity and invertibility of $P_t - P_{t-1}$).

We aim at achieving the decomposition of P_t into orthogonal components, $P_t = P_t^* + \epsilon_t$, where P_t^* is the low-pass component and ϵ_t is the high-pass component. The component P_t^* is obtained by the application of a low-pass filter whose gain function decreases monotonically from 1 to 0 as the frequency ranges from 0 to π. The frequency at which the gain is equal to 0.5 is referred to as the *cutoff frequency* of the filter and it will be denoted by ϑ_c. This terminology means that the filter will preserve to a large extent the fluctuations with periodicity larger than $\mathtt{p}_c = 2\pi/\vartheta_c$ and reduce the amplitude of those with smaller period (high-frequency variation).

Consider the following orthogonal decomposition of ξ_t:

$$\xi_t = \frac{(1+L)^s}{\varphi(L)}\eta_t + \sqrt{\varsigma}\frac{(1-L)^s}{\varphi(L)}\zeta_t,$$

where $\eta_t \sim \mathrm{WN}(0, \sigma^2), \zeta_t \sim \mathrm{WN}(0, \sigma^2)$, and $\mathrm{E}(\eta_t \zeta_{t-j}) = 0, \forall j \in \mathbb{Z}$. The lag polynomial $\varphi(L)$ satisfies the relation

$$\varphi(L)\varphi(L^{-1}) = (1+L)^s(1+L^{-1})^s + \varsigma(1-L)^s(1-L^{-1})^s, \tag{8}$$

while the scale parameter ς is related to the cutoff frequency $\theta_c = 2\pi/\mathtt{p}_c$ by $\varsigma = \left(\frac{1+\cos\theta_c}{1-\cos\theta_c}\right)^s$. See ? (?) for further details. The factorization of the right hand side of (8) exists and is unique since its Fourier transform is strictly positive, see ? (?), who discuss a variety of algorithms for computing $\varphi(L)$, given s and ς.

Given a particular choice of s and $\mathtt{p}_c$, or equivalently θ_c, it can be shown that the lowpass and highpass components have respectively the following ARMA($p+s$, $q+s-1$) representations:

$$\Delta P_t^* = \mu + \frac{\theta(L)(1+L)^s}{\phi(L)\varphi(L)}\eta_t, \quad \epsilon_t = \sqrt{\varsigma}\frac{\theta(L)(1-L)^{s-1}}{\phi(L)\varphi(L)}\zeta_t,$$

(notice that the spectral density of ΔP_t^* is zero at the Nyquist frequency, corresponding to a period of 2 days, whereas that of ϵ_t is zero at the long run frequency).

The minimum mean square linear estimator of P_t^* based on a doubly infinite sample $P_{t-j}, j = -\infty, -1, 0, 1, \ldots, \infty$, is $\hat{P}_t^* = w_{LP}(L)P_t$, where $w_{LP}(L)$ is the Wiener-Kolmogorov low-pass filter

$$w_{LP}(L) = \frac{(1+L)^s(1+L^{-1})^s}{\varphi(L)\varphi(L^{-1})},$$

see ? (?). Given a finite realization of P_t, the estimation of P_t^* is carried out by representing the decomposition as a state space model and applying the Kalman filter and smoother, see ? (?). Hence, even though $w_{LP}(L)$ does not depend on the autoregressive and moving average parameters, the finite sample properties (the behaviour of the boundaries of the sample and the estimation error) will depend on the ARIMA model for P_t.

For the S&P500 stock index we fitted the ARIMA(0,1,1) model $\Delta P_t = \mu + \xi_t + \theta\xi_{t-1}$ to the series from Jan. 3 2000 to Aug. 30, 2023; the parameter estimates resulted $\hat{\mu} = 1.80 \times 10^{-4}$ (s.e. 1.49×10^{-4}, $\hat{\theta} = -0.11$ (s.e. 0.01), $\hat{\sigma} = 0.0124$. Figure 9 displays the estimates of the low-pass component of the price series, p_t, corresponding to cutoff frequencies corresponding to periods equal to 5 days (red line) and 22 days (blue line), for the subperiod January 3, 2023 - August 30, 2023. The corresponding drawdown, evaluated on the smoothed series, is plotted in the lower panel. It can be seen that using $\theta_c = 2\pi/22$ provides a smooth assessment of the drawdown and that the series is zero more often when high-frequency variation is removed. A less desirable feature is the reduction of the size of the drawdown, which is an unavoidable consequence of smoothing the price series. A

Figure 9: Logarithm of S&P500 closing price (January 3, 2023 - August 30, 2023). Estimates of the low-pass components of prices and drawdown with cutoff frequency $2\pi/5$ and $2\pi/22$.

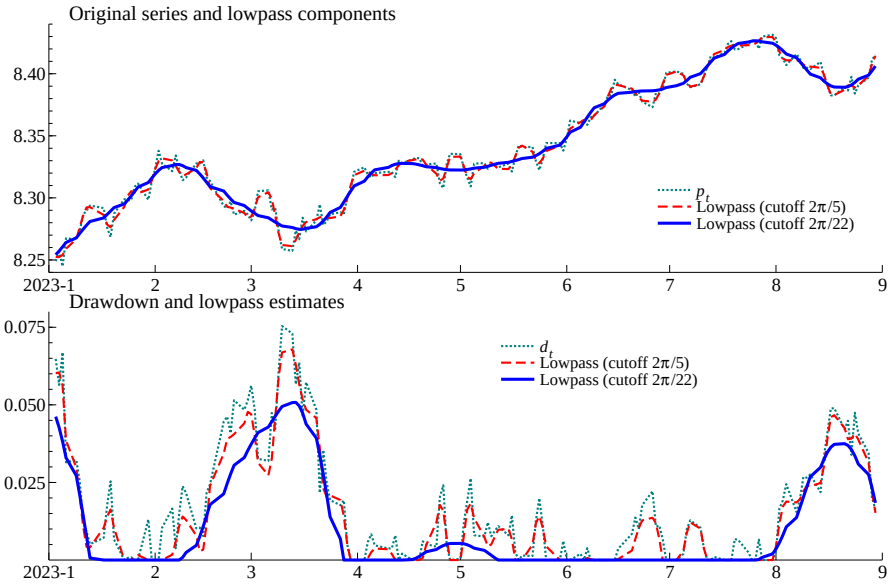

solution that avoids this potential drawback and that gets close to the censoring approach proposed by ? (?) is to estimate the drawdown by $d_t I(\tilde{d}_t > 0)$, where $\tilde{d}_t$ is the drawdown evaluated for the lowpass component of p_t.

8 Conclusions

The measurement approach considered in this paper generates, along with the drawdown and drawup, two Markov processes measuring the current lag with respect to the running maximum and minimum, that serve the purpose of characterizing the time series properties (persistence, duration, etc.) of the drawdown and drawup. They are at the basis of a novel model-free dating algorithm for bear and bull phases that is computationally efficient and easy to implement.

This paper has proposed a unifying framework that integrates conventional time series techniques with the measurement approach discussed above to address tasks such as robust estimation and drawdown prediction. In particular, it has demonstrated that

the support of a parametric dynamic model for asset prices facilitates both point and density forecasting of the drawdown process. Moreover, by disentangling microstructure or high-frequency variation from the underlying price dynamics, the model enables robust estimation of drawdowns and a formal assessment of the uncertainty surrounding the dating of financial cycle phases. The latter can be achieved by simulating multiple paths from the distribution of latent prices conditional on observed prices, using conditional simulation, filtering, and smoothing methods (?, ?). The probability of being in a bull or bear phase can then be estimated as the fraction of Monte Carlo paths that correspond to that state.

Availability of Data and Materials

The time series used in this paper are S&P500 daily stock market index (closing price) from January 3, 2000, to August 30, 2023, and its components stocks. The time series were downloaded from Yahoo Finance using the `quantmod` R package and the tickers obtained from Wikipedia's *List of S&P 500 companies*.

Acknowledgments

A preliminary version of this paper was presented at the International Symposium on Nonparametric Statistics 2024, June 25-29, 2024 - Braga, Portugal, and at the 44th International Symposium on Forecasting, June 30 - July 3, 2024 - Dijon, France, under the title *Measuring and Predicting Cyclical Turning Points, Gaps, and Drawdowns.* The author gratefully acknowledge financial support by the Italian Ministry of Education, University and Research, Progetti di Ricerca di Interesse Nazionale, research project 2020-2023, prot. 2020N9YFFE.